

(1) Apollo Passive Seismic Experiment Seismometer

(System) [1],[2]

The Apollo Passive Seismic Experiment Seismometer consists of two main subsystems; the sensor unit and the electronics module. The sensor contains three matched long-period (LP) seismometers alined orthogonally to measure one vertical (LPZ) and two horizontal components (LPX, LPY) of surface motion. The sensor also includes a single-axis short-period (SP) seismometer sensitive to vertical motion at higher frequencies.

The instrument is constructed principally of beryllium and weighs 11.5 kg, including the electronics module and thermal insulation (aluminized Mylar). Without insulation, the sensor is 23 cm in diameter and 29 cm in high. Total power drain varies between 4.3 and 7.4 W. Instrument temperature control is provided by a 2.5-W heater, a proportional controller, and an insulating wrapping of aluminized Mylar. The insulating shroud is spread over the local surface to reduce temperature variations of the surface material. In this way, it is expected that thermally induced tilts of the local surface will be reduced to acceptable levels.

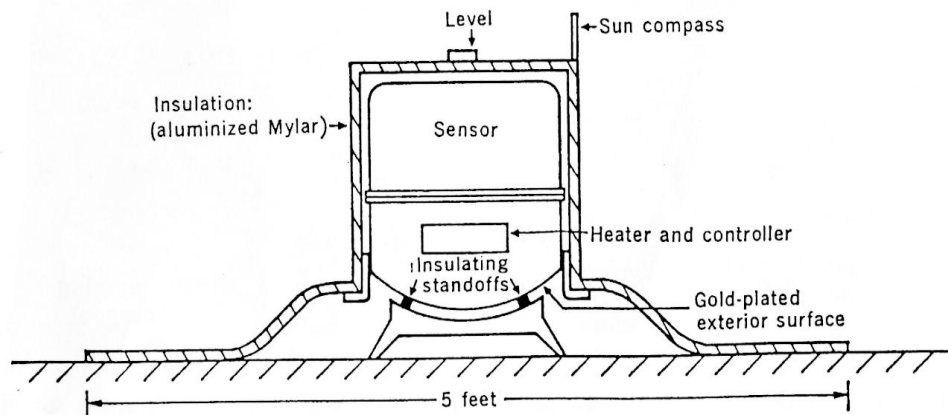


Fig. 1 Schematic diagram of the PSE seismometer [1]

① LP (Long-Period Sensor)

[Description] ([3])

Long-period seismometer (LP) has resonant periods of about 15 sec and three closely matched orthogonal, pendulums. A LaCoste type spring is used for the suspension of the mass in the vertical long-period seismometer (Z), while the horizontal sensors (X and Y) employ a swinging-gate system. Since the relative motion between the mass and the frame of the long-period is measured by capacitor-type displacement transducers, the electrical output is proportional to the relative displacement between the mass and frame. Long-term stability of the instruments is accomplished by feedback circuits, which can be switched between the normal (flat) and the

modified (peaked) modes of operation. In the latter mode, the feedback filter is bypassed and the transfer function was sharply peaked at a period of about 2.2 sec.

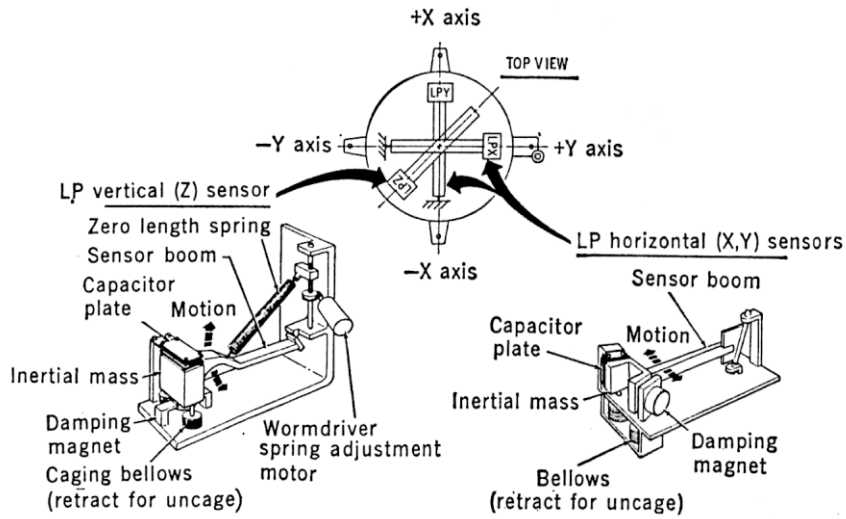


Fig.2. Sensor pendulums of the Apollo LP seismometer [1]

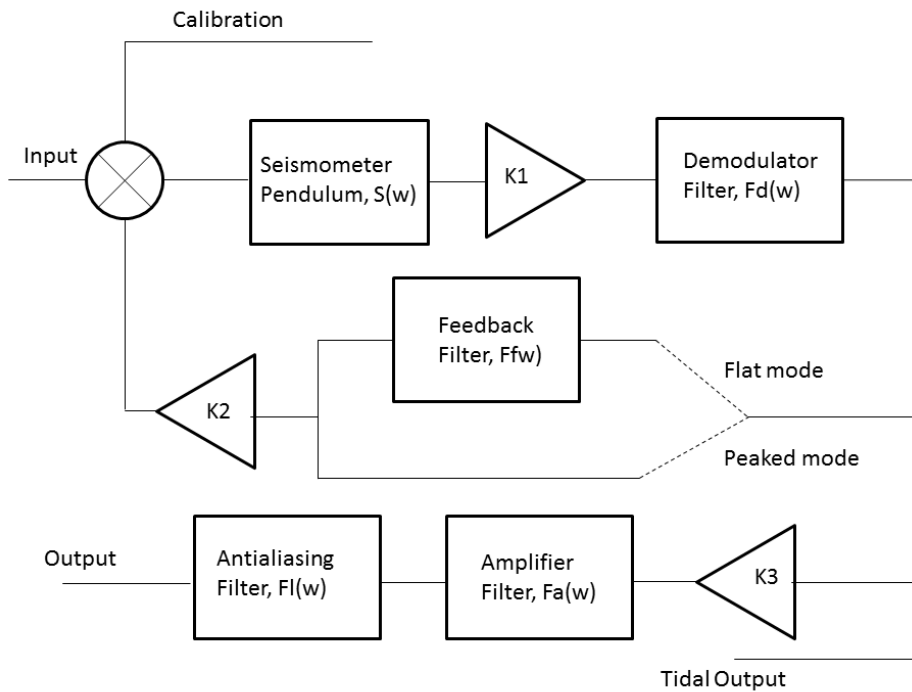


Fig.3 Block diagram of LP seismometer with feedback circuit [3]

[Response] [3]

① Flat mode

As shown in Figure 3, the response of LP with flat mode $AF(\omega)$ for acceleration is represented by

$$AF(\omega) = K_{3*}F_a(\omega) * Fl(\omega) * Fs(\omega) \text{ (V/m/sec}^2\text{)}$$

where ω is angular frequency, and K_3 is amplifier gain of feedback output. Then, $F_a(\omega)$ is the transfer function of the 1-st order high-pass filter in the output amplifier,

$$F_a(\omega) = \frac{s}{\omega_a + s}$$

$$s = i\omega$$

where ω_a is output high pass cut-off angular frequency. $Fl(\omega)$ is the transfer function of the output low-pass antialiasing filter,

$$AF(\omega) = K_{3*}F_a(\omega) * Fl(\omega) * Fs(\omega)$$

$$Fl_a(\omega) = \frac{\omega_l^2}{s^2 + 2i\cos\left(\frac{\pi}{8}\right)\omega_l\omega + \omega_l^2}$$

$$Fl_b(\omega) = \frac{\omega_l^2}{s^2 + 2i\cos\left(\frac{3\pi}{8}\right)\omega_l\omega + \omega_l^2}$$

where, ω_l is output low pass cut-off angular frequency. Then, $F_s(\omega)$ is the transfer function of feedback component of the seismometer and the response is represented by

$$F_s(\omega) = \frac{K_1S(\omega)F_d(\omega)}{1 + K_1K_2S(\omega)F_d(\omega)F_f(\omega)}$$

In here, K_1 is the gain of displacement transducer in (V/m), and K_2 is the coil-magnet transfer function in (m/sec²/V). $S(\omega)$ is the transfer function of the seismometer for acceleration and the output is the displacement between the seismometer mass and the frame,

$$S(\omega) = \frac{1}{s^2 + 2h\omega_0s + \omega_0^2}$$

$$\omega_0 = 2\pi f_0$$

where, f_0 is the resonant frequency of the pendulum and h is the damping constant.

$F_d(\omega)$ is the transfer function of the demodulator low-pass filter, and represented by

$$F_d(\omega) = \frac{\omega_d}{s + \omega_d}$$

where ω_d is the demodulator low pass cut off angular frequency. $F_f(\omega)$ is the transfer function of the feedback low-pass filter,

$$F_f(\omega) = \frac{\omega_f}{s + \omega_f}$$

where ω_f is the feedback low pas cut off angular frequency.
The value of each parameter is substituted by

$$K_1 = 500000 \text{ (V/m)}$$

$$K_2 = 0.000016 \left(\frac{\text{m/sec}^2}{\text{V}} \right)$$

$$K_3 = 31.6$$

$$\omega_a = 0.0628 \text{ (rad)}$$

$$\omega_l = 8.72665 \text{ (rad)}$$

$$f_0 = 0.06667 \text{ (Hz)}$$

$$h=0.85$$

$$\omega_d = 47.62 \text{ (rad)}$$

$$\omega_f = 0.000997 \text{ (rad)}$$

If we want to covert the response of LP to that for displacement in (V/m), we have to multiply $AF(\omega)$ by square of Laplace function s,

$$AF \text{ (V/m)} = s^2 * AF$$

Then unit of $AF(\omega)$ is converted to (DU/m) from (V/m) using the reciprocal value of 1LSB of AD converter in Apollo seismometer electronics,

$$K = 204.9 \text{ (DU/V)}$$

② Peaked mode

As shown in Figure 3, the response of LP with peaked response mode $AP(\omega)$ is represented by eliminating the transfer function of the feedback low-pass filter $F_f(\omega)$ from equation of $AF(\omega)$,

$$AP(\omega) = K_3 * F_a(\omega) * Fl(\omega) * F_s'(\omega) \text{ (V/m/sec}^2\text{)}$$

$$F_s'(\omega) = \frac{K_1 S(\omega) F_d(\omega)}{1 + K_1 K_2 S(\omega) F_d(\omega)}$$

The unit of $AP(\omega)$ is converted to (DU/m) from (V/m/sec²) using square of Laplace function and the reciprocal value of 1LSB of Apollo-AD such as the response of flat-mode.

③ Tidal mode

Tidal mode outputs the unfiltered and unamplified feedback signal proportional to long-period boom motion. This signal gives tidal tilts and changes in the magnitude of gravity. The tidal mode response $TD(\omega)$ is represented by

$$TD(\omega) = F_5(\omega) \text{ (V/m/sec}^2\text{)}.$$

The effects of output amplifier and filters $K_3, F_a(\omega), Fl(\omega)$ are all removed in this mode.

(1) SP (Short-Period Sensor)

[Description] ([2],[3])

In the short-period instrument, a moving magnet mass is suspended from the frame with a LaCoste spring as the main support element and “delta rods” in a triangular configuration to keeping mass centered. By its movement, this magnet induces voltage in coil, which is fixed to the frame. This voltage is therefore proportional to the relative velocity between the frame and the suspended mass.

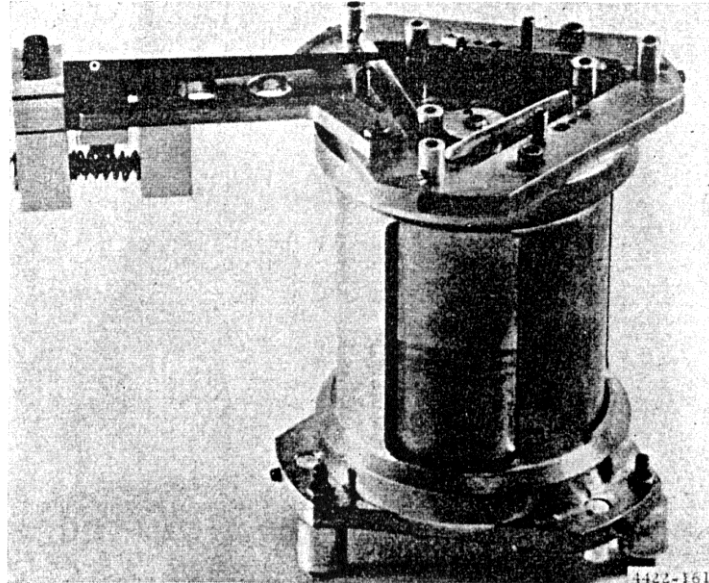


Fig.4 Breadboard model of the Apollo SP seismometer [2]

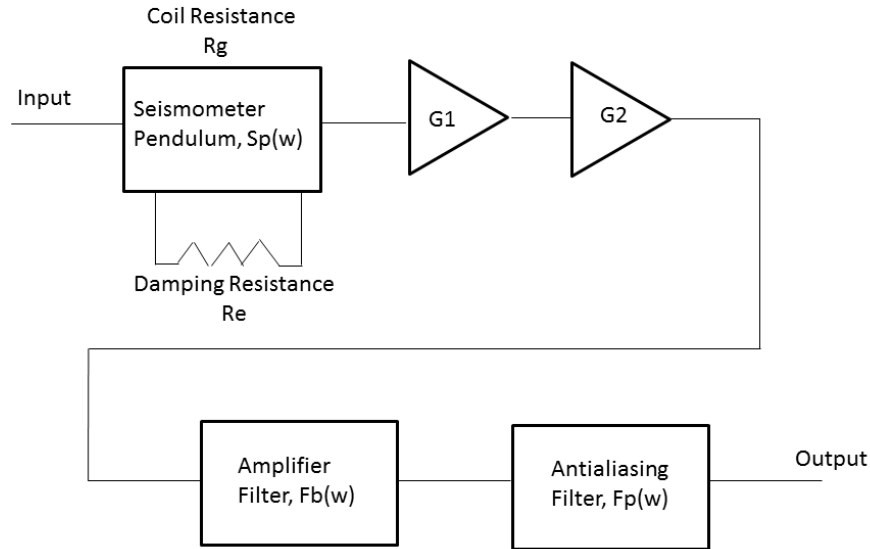


Fig.5 Block diagram of SP seismometer

[Response] (Nakamura, 2010 personal communication)

As shown in Fig. 5, the response of the Apollo SP seismometer $ASP(\omega)$ is represented by

$$ASP(\omega) = G * G_1 * G_2 * S_p(\omega) * F_b(\omega) * F_p(\omega) \text{ (V/m/sec}^2\text{)}$$

where G is the damping controlled gain, and is represented by

$$G = \frac{R_e}{R_g + R_e}$$

using R_g : coil resistance and R_e : damping resistance in ohm. G_1 is generator constant of the magnet-coil system in (V/m/sec) and G_2 is pre-amplifier gain.

$S_p(\omega)$ is the transfer function of the short-period sensor for acceleration and the output is the velocity between the seismometer mass(moving magnet) and the frame (fixed coil),

$$S_p(\omega) = \frac{s}{s^2 + 2h\omega_0 s + \omega_0^2}$$

$$\omega_0 = 2\pi f_0$$

where, f_0 is the resonant frequency of the pendulum and h is the damping constant. $F_b(\omega)$ is the transfer function of the 1-st order high-pass filter in the output amplifier,

$$F_b(\omega) = \frac{s}{\omega_b + s}$$

where ω_b is output high pass cut-off angular frequency.

$F_p(\omega)$ is the transfer function of the output low-pass antialiasing filter,

$$F_p(\omega) = (F_{pa}(\omega))^2 * (F_{pb}(\omega))^2$$

$$F_{pa}(\omega) = \frac{\omega_p^2}{s^2 + 2i\cos\left(\frac{\pi}{8}\right)\omega_p\omega + \omega_p^2}$$

$$F_{pb}(\omega) = \frac{\omega_p^2}{s^2 + 2i\cos\left(\frac{3\pi}{8}\right)\omega_p\omega + \omega_p^2}$$

where, ω_p is output low pass cut-off angular frequency.

The value of each parameter is substituted by

$$R_g = 1800 (\Omega)$$

$$R_e = 2680 (\Omega)$$

$$G_1 = 175 (V/m/sec)$$

$$G_2 = 23700$$

$$f_0 = 1.0 (Hz)$$

$$h = 0.85$$

$$\omega_b = 0.31416 (\text{rad})$$

$$\omega_p = 57.1199 (\text{rad})$$

If we want to represent the response of SP as that for displacement in (V/m), we have to multiply $ASP(\omega)$ by square of Laplace function s ,

$$ASP(\omega)(V/m) = s^2 * ASP(\omega)$$

Then unit of $ASP(\omega)$ is converted to (DU/m) from (V/m) using the reciprocal value of 1LSB of Apollo-AD,

$$K = 204.9 (DU/V)$$

[Response-curves]

The response curves of Apollo LP (flat and peaked modes), tidal mode and Apollo SP for displacement are shown in Fig. 6.

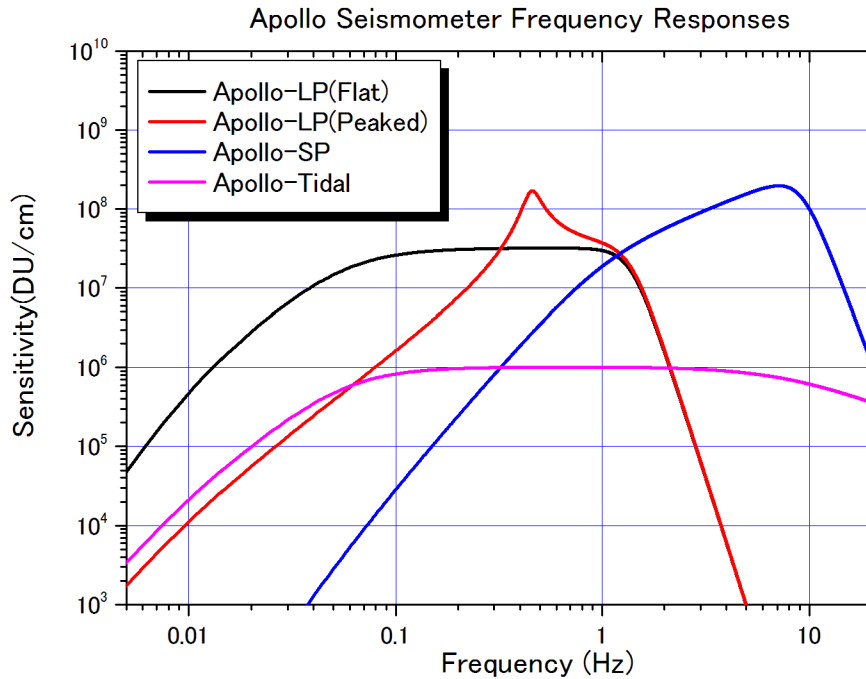


Fig.6 The response curves of the Apollo seismometers

(2) Apollo Active Seismic Experiment

[Description] ([4],[5])

Apollo Active Seismic Experiments (ASE) has been performed at Apollo 14, 16. In this experiment, three identical geophones were used. The geophones are miniature seismometers of the moving coil-magnet type. The coil is the inertial mass suspended by springs in the magnetic field. Above the natural resonant frequency of the geophones (7.5 Hz), the output is proportional to ground velocity.

[Response]

The characteristics and response curves of the geophones on Apollo 14 and 16 sites are indicated below.

① Apollo 14-ASE

Apollo 14 ASE Geophone Characteristics [4]

Characteristics Component	Geophone No.		
	Geophone 1	Geophone 2	Geophone 3
Resonant frequency (Hz)	7.32	7.22	7.58
Generator constant (V/m/sec)	250.4	243.3	241.9
Coil resistance (Ω)	6065	6157	6182
Amplifier Noise level (μV rms at input)	0.3	0.325	0.272
Amplifier Gain (at 10Hz and $V_{\text{input}}=0.0005\text{V}$ rms)	666.7	666.7	675.7
Dynamic range, rms signal to rms noise (dB)	86.8	86.5	87.5
System signal to noise ratio (rms signal to noise in dB for 1-nm peak-to-peak signal at 10Hz)	33.6	33.1	32.9

The response curve for geophone sensor $GR(\omega)$ is represented by following equation;

$$GR(\omega) = A * GS(\omega)$$

where, A is the amplifier gain and $GS(\omega)$ is the transfer function of the geophone pendulum for velocity and the output means the relative velocity between the seismometer mass(moving coil) and the frame (fixed magnet),

$$GS(\omega) = \frac{G * s^2}{s^2 + 2h\omega_0 s + \omega_0^2}$$

$$\omega_0 = 2\pi f_0$$

In this equation, f_0 is the resonant frequency of the pendulum, h is the damping constant and G is the generator constant of the sensor.

The response curves of the geo-phones used for ASE at site 14 are indicated in Figure 7. In these curves, I assume that the damping constant h of 0.50 and the antialiasing low-pass filter with cut-off frequency of 150 Hz. The sampling rate of ASE geo-phone at site 14 is 530 Hz. The low signal-to-noise ratios expected and the lack of knowledge as to the character of the expected waveforms made it desirable to widen the frequency response as much as possible within the constraints of the digital sampling frequency [4].

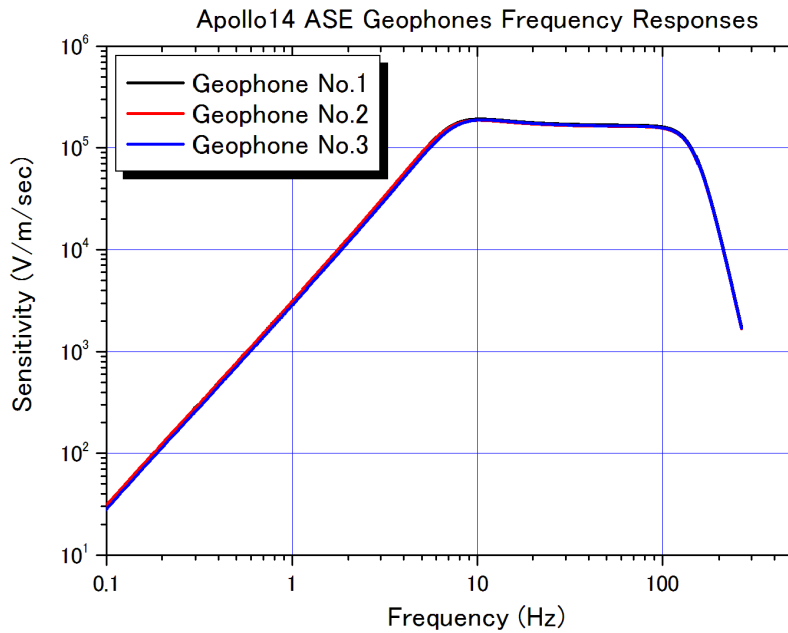


Fig.7 The response curves of Apollo14 ASE geo-phones

② Apollo16-ASE

Apollo 16 ASE Geophone Characteristics [5]

Characteristics Component	Geophone No.		
	Geophone 1	Geophone 2	Geophone 3
Resonant frequency (Hz)	7.42	7.44	7.39
Generator constant (V/m/sec)	255	255	257
Coil resistance (Ω)	6090	6212	6204
Amplifier Noise level (μV rms at input)	0.266	0.100	0.133
Amplifier Gain (at 10Hz and $V_{\text{input}}=0.0005\text{V}$ rms)	698	684	709
Dynamic range, rms signal to rms noise (dB)	84.4	92.4	90
System signal to noise ratio (rms signal to noise in dB for 1-nm peak-to-peak signal at 10Hz)	38.9	37.9	45.0

The equations of frequency responses of geophone at site 16 are same as that at site 14. The response curves of the geo-phones used for ASE at site 16 are indicated in Figure 8 using the parameters listed on above table. The sampling rate of ASE geo-phone at site 16 is 530 Hz

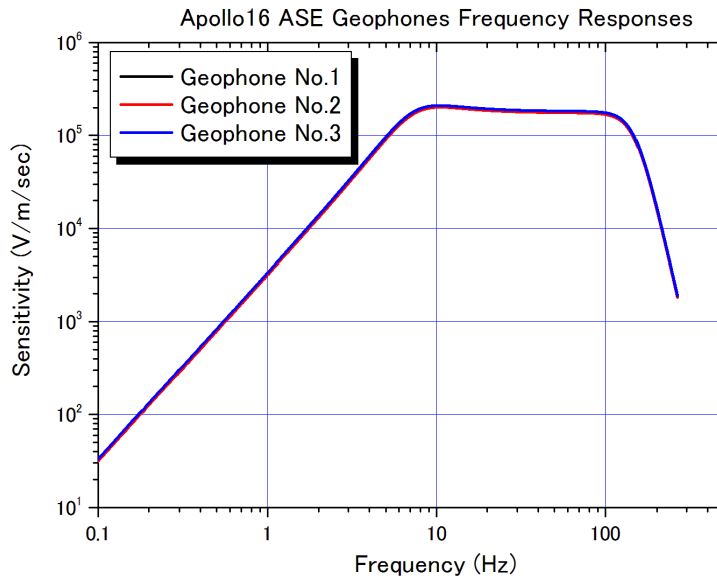


Fig.8 The response curves of Apollo16 ASE geo-phones

[Data Conversion] ([6])

Because the signal levels of ASE were distributed throughout the dynamic range of the system, logarithmic compressor was used to archive the maximum dynamic range. This compression gives signal resolution as some constant fraction of signal amplitude.

In the ASE, the seismic data were log compressed into 32 binary levels. The binary data in the geophone No.1, 2 and 3 must be decompressed to obtain the actual seismic signal data from the geophones.

The appropriate expansion formula to recover true input voltage V_{in} (output voltage from a geophone and pre-amplifier) from the output voltage of the logarithmic compressor V_{out} is

$$V_{in} = \frac{V_{out} - 2.420}{V_3}$$

if $2.170 < V_{out} < 2.670$,

for decimal 14, 15 and 16; and

$$V_{in} = \pm \exp \frac{V_{out} - V_1}{\pm V_2}$$

for decimal 0 to 13 and 17 to 31; the + sign is used for positive input signal and the – sign is used for negative input signals.

The values of V_1 , V_2 (positive and negative) and V_3 for the Apollo 14 and 16 systems are derived from the calibration data supposed from Dr. Yoshio Nakamura. These values are listed in below tables. (Nakamura, 2010, personal communication)

	Station 14 Geophones		
	No.1	No.2	No.3
V1+ (decimal 0 to 13)	4.55135	4.55342	4.55694
V1- (decimal 17 to 31)	0.29296	0.28192	0.27628
V2+ (decimal 0 to 13)	0.27046	0.26984	0.27088
V2- (decimal 17 to 31)	-0.26996	-0.26996	-0.27128
V3	332	332	332

	Station 16 Geophones		
	No.1	No.2	No.3
V1+ (decimal 0 to 13)	4.55780	4.55798	4.55303
V1- (decimal 17 to 31)	0.28260	0.30123	0.26124
V2+ (decimal 0 to 13)	0.26773	0.27065	0.26813
V2- (decimal 17 to 31)	-0.26858	-0.26983	-0.27054
V3	332	332	332

Then, the log-compressed output V_{out} is converted to the 32 binary levels (Digital unit) as shown in below table. Compression is linear if V_{out} is between 2.170 and 2.670 Volts.[6]

DU	Vout	
0	0.05906	Negative Input Signals
1	0.21654	
2	0.37402	
3	0.53150	
4	0.68898	
5	0.84646	
6	1.00394	
7	1.16142	
8	1.31890	
9	1.47638	
10	1.63386	
11	1.79134	
12	1.94882	
13	2.10630	
14	2.26378	
15	2.42126	
16	2.57874	Positive Input Signals
17	2.73622	
18	2.89370	
19	3.05118	
20	3.20866	
21	3.36614	
22	3.52362	
23	3.68110	
24	3.83858	
25	3.99606	
26	4.15354	
27	4.31102	
28	4.46850	
29	4.62598	
30	4.78346	
31	4.94094	

(3) Lunar Seismic Profiling Experiment

[Description] (7)

The Lunar Seismic Profiling Experiment (LSPE) was performed at Apollo 17 site. The experiment consists of a geophone array, eight explosive package, and electronics within the Apollo lunar surface experiments package (ALSEP) central station. Four identical geophones are used in a triangular array; the geophones are miniature seismometers of the moving coil-magnet type. The coil is the inertial mass suspended by springs in the magnetic field. Above the natural resonant frequency of the geophones (7.5Hz), the output is proportional to ground velocity. These seismometers are same types to those used in ASE at Apollo 14, 16 sites. The seismic data in LSPE was recorded with the sampling frequency of 117.78(Hz). These geophones were also used for Passive Listening Mode in this experiment.

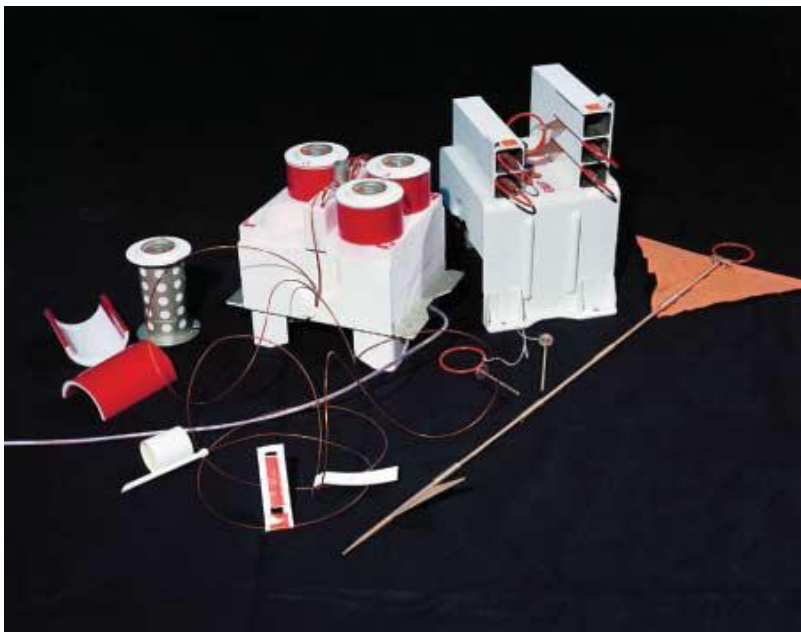


Fig.9 The four geophones used for Apollo 17 Lunar Seismic Profiling Experiments [8]

[Response]

The characteristics of the four geophones used in Lunar Seismic Profiling Experiment are indicated below. Then, the response curves of geophones used for LSPE are indicated in Figure 10. In these curves, I assume that the damping constant h of 0.70 and the antialiasing low-pass filter with cut-off frequency of 30 Hz.

Apollo 17 ASE Geophone Characteristics [7]

Characteristics Component	Geophone No.			
	Geophone 1	Geophone 2	Geophone 3	Geophone 4
Resonant frequency (Hz)	7.38	7.31	7.40	7.35
Generator constant (V/m/sec)	235.6	239.2	237.1	235.5
Coil resistance (Ω)	5970	5953	6080	6153
※Amplifier gain (at 10Hz)	495.2	467.1	477.9	482.3
Amplifier Noise level (mV rms at input)	0.75	0.75	0.83	0.83
Dynamic range, rms signal to rms noise in dB at 10 Hz	73.4	76.2	75.6	75.8
System signal to noise ratio (rms signal to noise in dB for 6-nm rms signal at 10 Hz)	24.4	26.9	26.8	26.8

※ In this table, amplifier gains were estimated from [LPSE system sensitivity] at 10 Hz indicated in Apollo 17 Preliminary Science Report [7]

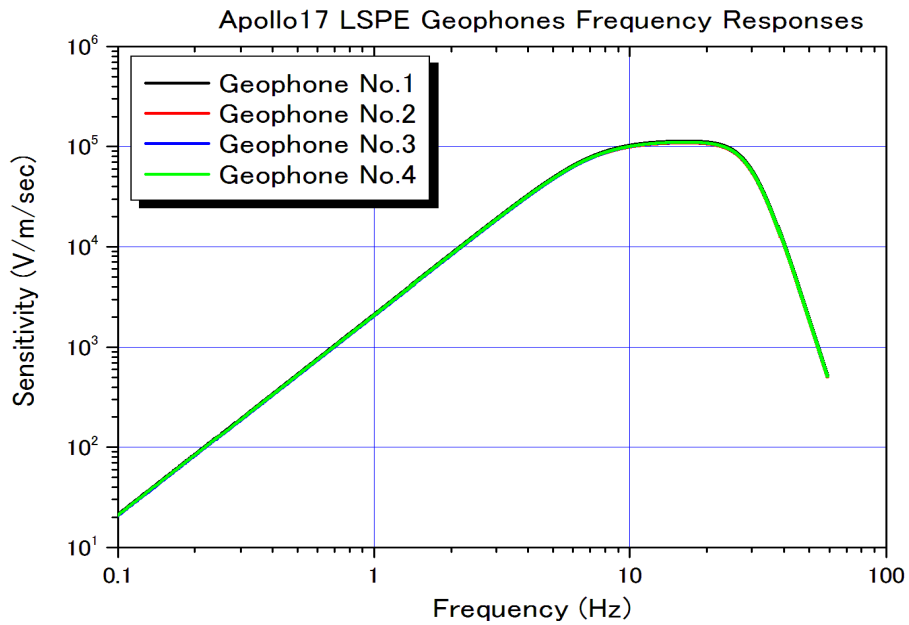


Fig.10 The response curves of Apollo17 LSPE geophones

[Data Conversion]

A four-channel amplifier and a logarithmic compressor condition the geophone signals before conversion into a digital format for telemetering to Earth. Because the signal levels of LSPE were distributed throughout the dynamic range of the system, logarithmic compressor was used to archive the maximum dynamic range. This compression gives signal resolution as some constant fraction of signal amplitude. The logarithmic compressor used in the LSPE has the transfer function;

$$V_{out} = \pm M * \ln|V_{in}| + b$$

where **V** is voltage, the constant **M** determines the slope of the transfer function, and **b** is specified by the dc offset of the compressor output and the system noise level. [7]

The values **M** of and **b** are determined from calibration data proposed by Dr. Yoshio Nakamura.

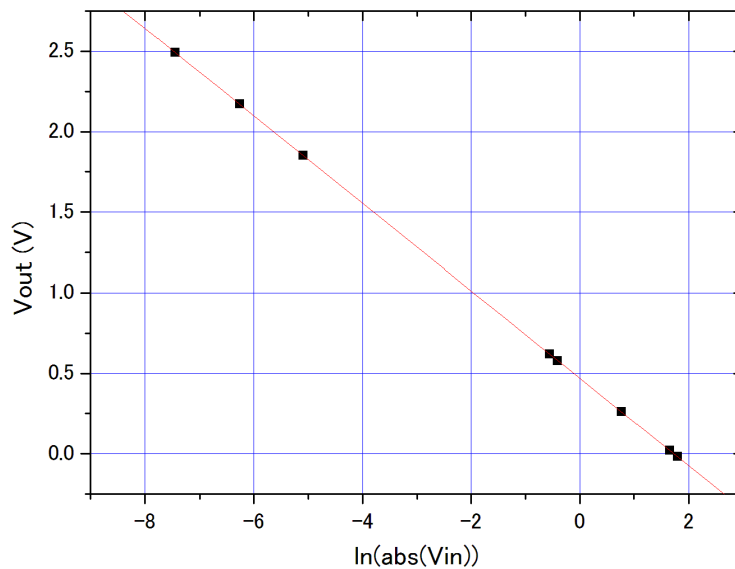


Fig.11 Relation between input and output voltages of the logarithmic compression in negative input voltage region

Figure 11 indicates the calibration data of logarithmic input voltage and output voltage of the logarithmic compression in negative input voltage region. I fitted the straight line into the data to derive the values of **M** and **b**. Then,

$$M = -0.2715 \pm 8.187E - 6$$
$$b = 0.4698 \pm 3.272E - 5.$$

On the other hand, the values of **M** and **b** are derived in the positive input voltage region using the similar way.

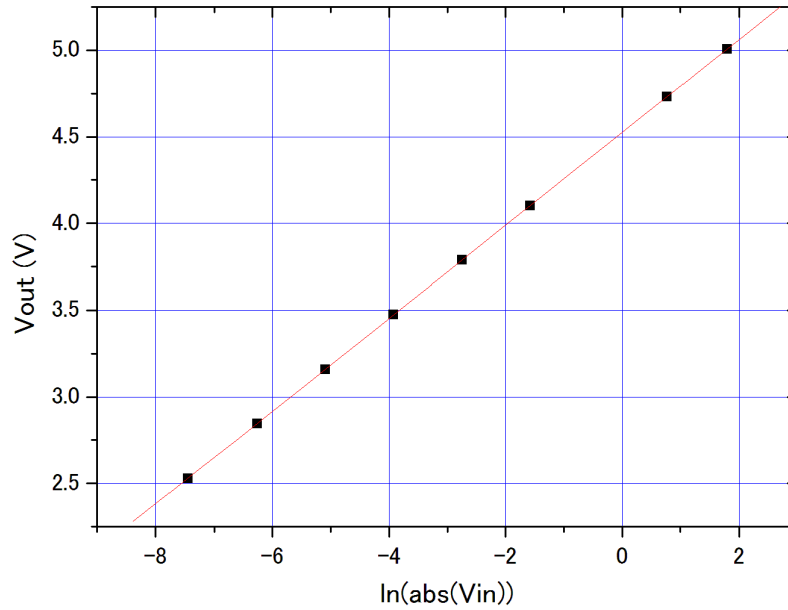


Fig.12 Relation between input and output voltages of the logarithmic compression in positive input voltage region

From the fitting shown in Figure 12,

$$M = 0.2681 \pm 7.086E - 6$$

$$b = 4.5260 \pm 3.068E - 4$$

Using these parameters, we can convert the output voltages of the geophone sensors to that of the logarithmic compression.

The analog output of the logarithmic compressor was converted to a 8-bit binary element in the LSPE control electronics by an analog-digital converter such as

$$D_{out} = K_g * V_{out} + B$$

where, D_{out} is the digital output of the AD converter, K_g is the conversion coefficient between input voltage and output digital unit of the AD converter and B is the dc offset. Then, the digital data was transmitted to Earth through the ALSEP communications network.

The values of K_g and B are also derived from the calibration data of the voltage output of the logarithmic compressor and the digital output of the AD converter.

$$K_g = 25.2609 \pm 0.0235$$

$$B = 0.2876 \pm 0.0672$$

Using the values of K_g , B , M , b and the response functions of the geophones, we can convert the digital output data to the output voltages of the geophones and the velocity of ground motion.

(4) Apollo Lunar Surface Gravimeter (LSG)

[Description]([9], [10])

Lunar Surface Gravimeter (LSG) was emplaced on the Moon by the Apollo 17 crew to detect gravitational waves predicted by Einstein's general relativity theory and to measure tidal deformation of the Moon.

This instrument is a sensitive balance with a mass, spring, and lever system and with electronics for observation of accelerations in the frequency range from 0 to 16 Hz. The LSG has a nominal sensitivity of approximately one part in 10^{11} of lunar gravity.

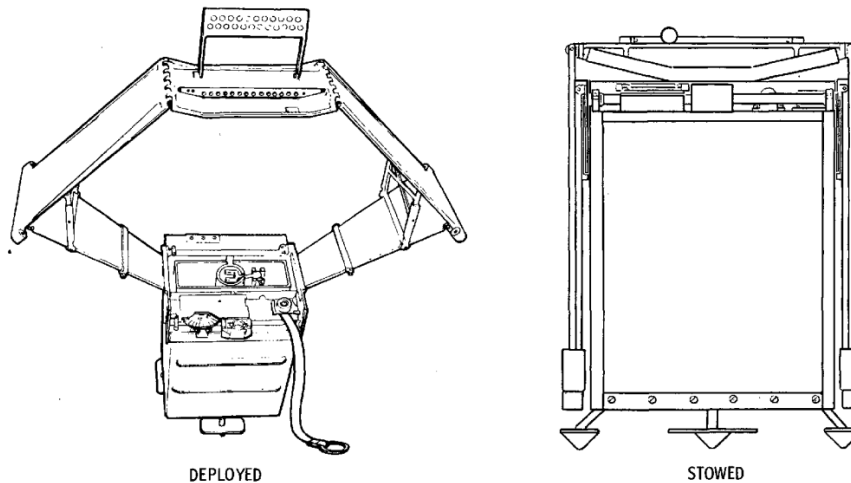


Fig.13 Schematic diagram of Lunar Surface Gravimeter Package [11]

In the instrument, the major fraction of the force supporting the sensor mass (beam) against the local gravitational field is provided by the zero-length spring. A zero-length spring is one in which the restoring force is directly proportional to the spring length; such spring is very useful in obtaining a long-period sensor. Small changes in force tend to displace the beam up or down. This imbalance is adjusted to the null position by repositioning the spring pivot points by use of micrometer screws. The sensor mass is modified by the addition or removal of small weights, permitting the range of the sensor to be extended from Earth testing to lunar operation. The electronic sensing portion of the instrument consists of a set of capacitor plates. Two plates, which are part of a radio-frequency bridge circuit, are fixed to the frame of the sensor and are geometrically concentric with a third plate of similar size, which is attached to the movable beam of the sensor. The plates are so arranged that the center plate is located exactly between the two outer plates when the beam is exactly horizontal. If the force on the mass changes, it tends to

move the beam, and the resulting bridge unbalance creates an AC error voltage. This voltage is amplified and rectified with the size of the output voltage determined by the direction of the displacement. A fixed DC bias voltage is applied to the capacitor plates balanced with respect to ground, and these plates are also connected to the rectified error voltage.

If the error voltage is zero, the balanced bias plate voltage produces equal and opposite electrostatic forces on the mass, if a positive error voltage is present, the voltage applied to one plate is increased and the voltage applied to the other plate is decreased. The resulting force tends to restore the mass to its originally centered position. This rectified voltage is a measure of the changes in surface acceleration. The mass does not follow fast changes. However, the fast-changing servomechanism error voltage is a measure of the rapidly changing components of the surface acceleration. A schematic diagram of the lunar gravity sensor is shown in Figure 14.

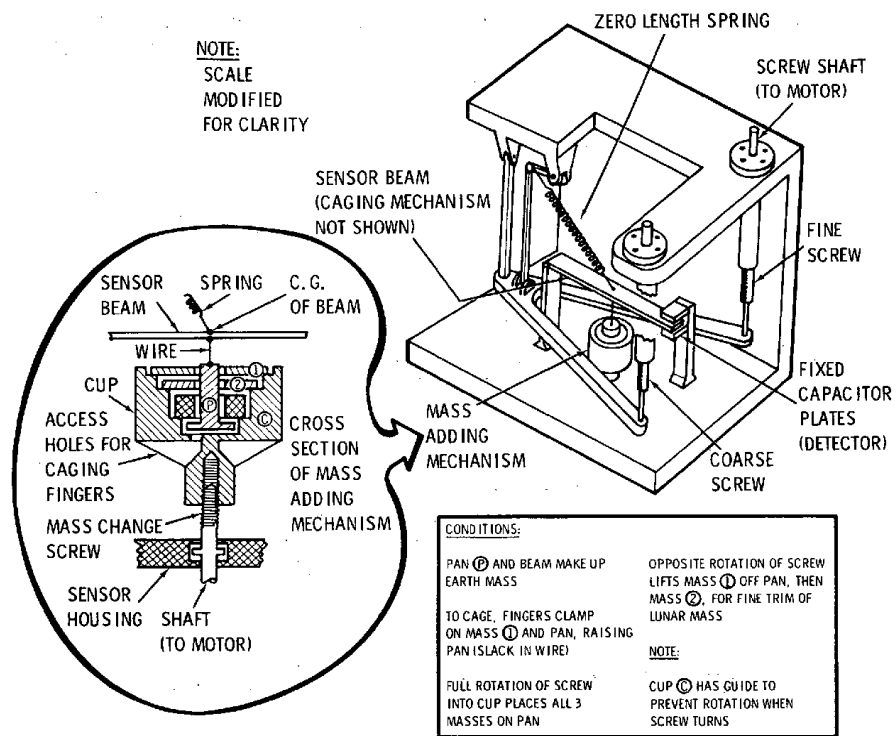


Fig.14 Schematic diagram of the lunar gravity sensor [11]

[Response] ([9],[12])

(Designed response)

The data cover the frequency range from 0 to 16 Hz in three bands (Free-mode, Tide-mode and Seismic mode). The rectified integrated error voltage over the range DC to 1 cycle per 20 min (0.000833Hz) gives information on the lunar tides. A filter with amplification covers the range from 1 cycle per 20 min to 1 cpm (0.01667Hz). Another filter amplifies the fast components in the range from 3 cpm 16 Hz. The latter range is of interest for seismology and for search for high-frequency gravitational radiation from sources such as the pulsars. The LSG can also be operated with the

voltage output not fed back to restore the beam to equilibrium. Figure 15 and 16 indicates block diagrams of the closed loop and open loop responses of LSG.

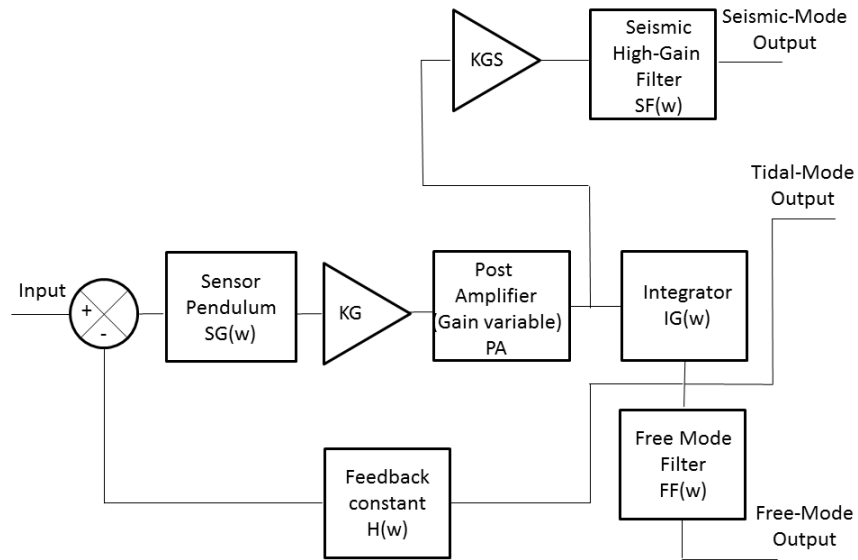


Fig.15 Block diagram of the LSG with closed loop operation [12]

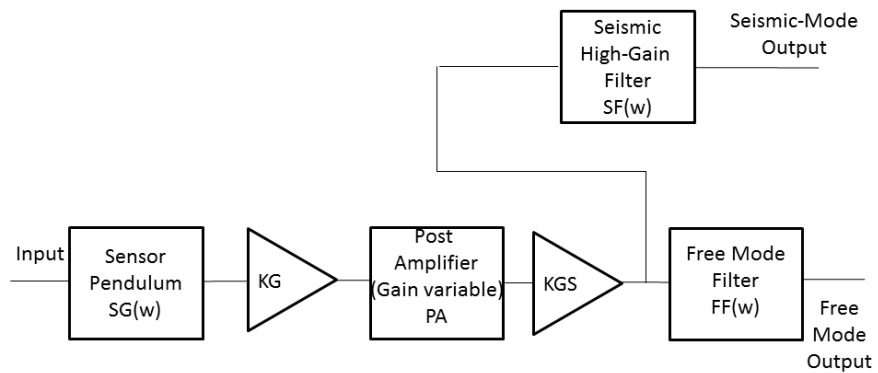


Fig. 16 Block diagram of the LSG with open loop operation [12]

As show in Figure 15 and 16, the transfer function of LSG with the free-mode $T_{fm}(\omega)$ in closed loop is represented by

$$T_{fm}(\omega) = FF(\omega) * \frac{KG * PA * SG(\omega) * IG(\omega)}{1 + H * KG * PA * SG(\omega) * IG(\omega)}$$

and that in open loop is

$$T_{fmo}(\omega) = FF(\omega) * KG * PA * KGS * SG(\omega)$$

where KG is sensitivity of displacement transducer in (V/m), PA is the post amplifier gain, and H is the feedback constant in (gals/volt), KGS is the seismic mode amplifier gain. PA is the variable gain from 1 to 86.4 in 16 discrete steps. Then, $SG(\omega)$ is the transfer function of the gravimeter pendulum for acceleration and the output is the displacement between the seismometer mass and the frame,

$$SG(\omega) = \frac{1}{s^2 + 2h\omega_0s + \omega_0^2}$$

$$\omega_0 = 2\pi f_0$$

where, f_0 is the resonant frequency of the sensor pendulum and h is the damping constant. $IG(\omega)$ is the transfer function of the integrator.

$$IG(\omega) = \frac{A}{1 + \tau_p s}$$

where, τ_p and A are the time constant and gain of the integrator. $FF(\omega)$ is the transfer function of the free mode filter. In this filter, I assume butter worth filter, and the parameters, degrees, gains and cut-off frequencies may be different for closed and open loop.

The LSG transfer function of the LSG with tidal mode $T_{td}(\omega)$ is represented by

$$T_{td}(\omega) = T_{fm}(\omega)/FF(\omega).$$

This transfer function is derived from dividing $T_{fm}(\omega)$ by the transfer function of the free mode filter in closed loop as shown in Figure 15.

The LSG transfer function of the LSG with seismic mode $T_{sm}(\omega)$ in closed loop is represented by

$$T_{sm}(\omega) = KGS * SF(\omega) * (T_{td}(\omega)/IG(\omega))$$

where $SF(\omega)$ is the transfer function of seismic high gain filter. I also assume the butter worth filter as this seismic filter. Then, the transfer function in the open loop $T_{smo}(\omega)$ is represented by

$$T_{smo}(\omega) = SF(\omega) * KG * PA * KGS * SF(\omega)$$

as shown in Figure 16.

The each parameter [12] of transfer function is substituted by

$$KG = 56.3 \text{ (V/m)}$$

$$KGS = 1.5$$

$$H = 10^{-4} \text{ (gals/V)}$$

$$f_0 = 0.04774 \text{ (Hz)}$$

$$h = 1.00$$

$$A = 500$$

$$\tau_p = 25000$$

The response curves of LSG with free and tidal modes for acceleration are indicated in Figure 17.

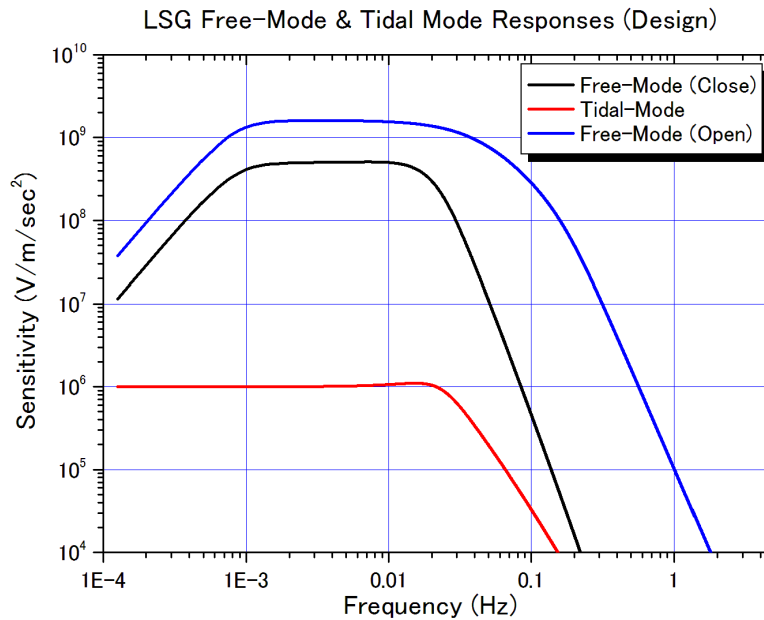


Fig. 17 The designed response curves of the LSG with free and tidal modes

In these curves, I used the values of higher cut-off frequency of 0.01677(Hz) and lower cut-off frequency of 0.00083 (Hz), gain of 500 and 2nd-order for the free-mode filter in closed loop. In

open loop, the higher cut-off frequency of 0.1677 (Hz) and gain of 250 for the free-mode filter are used. These values in the free-mode filter are derived so as to adjust the response curves indicated in [Lunar Surface Gravimeter Experiment] (Weber and Larson) [12].

In Figure 18, the response curves of the LSG with seismic mode for displacement are indicated.

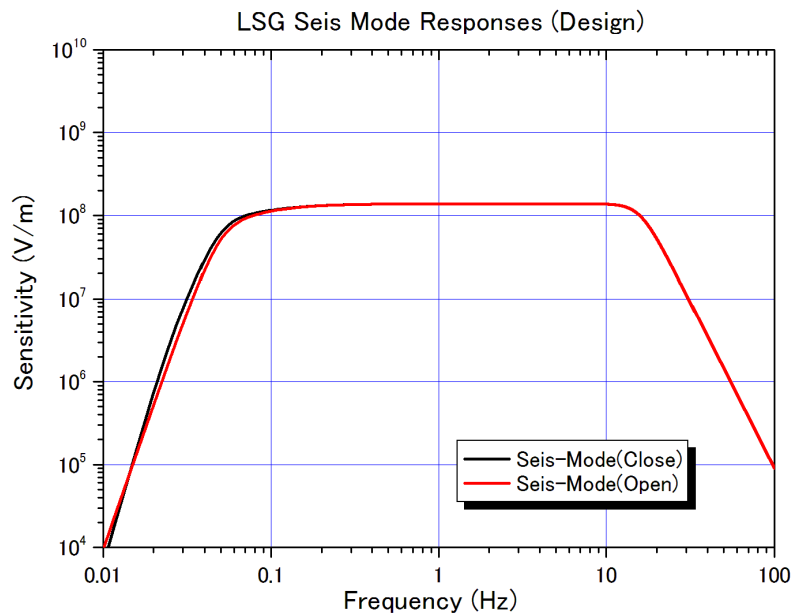


Fig.18 The designed response curves of the LSG with seismic mode

In these response curves, the values of higher and lower cut-off frequencies of 16 and 0.05 (Hz) are used for the seismic high gain filter. Then, the 4th-order and gain of 19000 are assumed in this filter. The maximum value of PA; 86.5 is used for the gain of post amplifier in Figs. 17 and 18.

(Actual Response)

On the other hand, the LSG at site 17 had never worked with the designed response, because the sensor mass was not located in the center position between capacitors in this frequency response. To balance the beam using a very small force applied by the mass adding mechanism, we have to change the frequency response of the sensor to significantly higher frequency than that originally intended. As a result, the natural frequency was lowered to approximately 1.5 Hz. In this higher frequency range, the damping factor Q ($1.0/2 \cdot h$) is in the order of 25. [10]

Figure 19 and 20 shows the response curves of the LSG with three modes used in actual observation. In these response curves, the resonant frequency of 1.90986 and the damping constant of 0.02 are used as actual value.

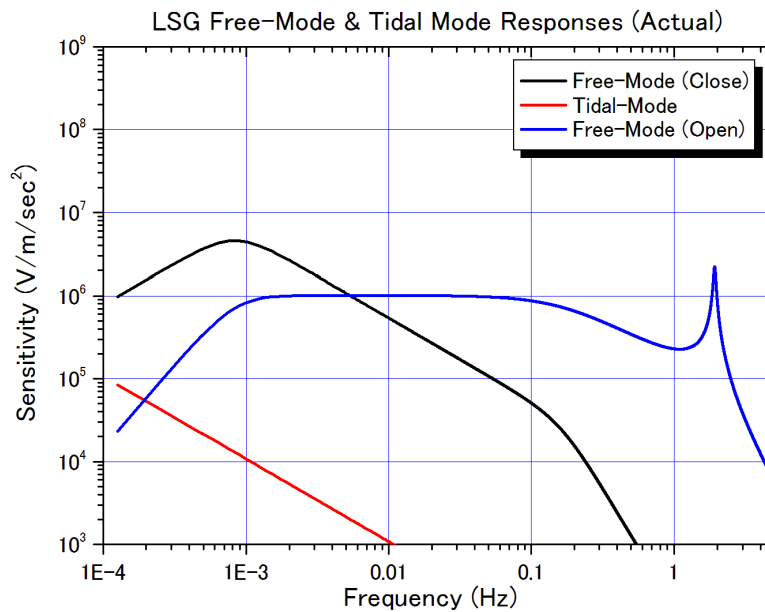


Fig.19 The actual response curves of the LSG with free and tidal mode.

In Fig. 19, higher cut-off frequency of 0.1667 (Hz) are used for the free-mode filter in closed loop. In open loop, order in higher frequency range is changed to 1st from 2nd.

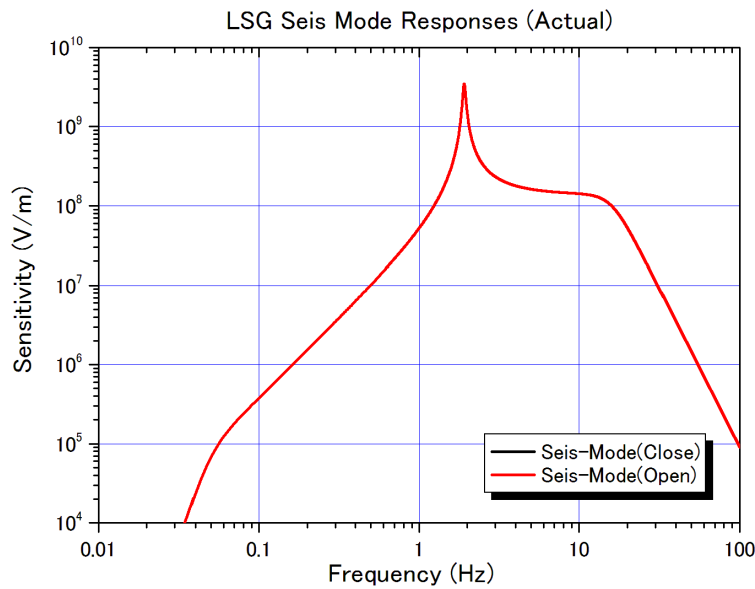


Fig. 20 The actual response curves of the LSG with seismic mode

Figure 20 shows that the LSG with seismic mode has worked as the narrow-band seismometer around the frequency range of 1Hz.

The value of 1LSB of LSG-A/D is 20 (mV). Using this value, we can convert the unit of the sensitivity to (DU/cm) from (V/m) and (V/m/sec²) so as to compare with the responses of the Apollo PSE. In this retrieval system, the data of LSG during March 1, 1976 and Sept. 30, 1977 is archived. During this period, the LSG has worked with open loop. Figure 21 shows the open loop response curves of the LSG with three modes.

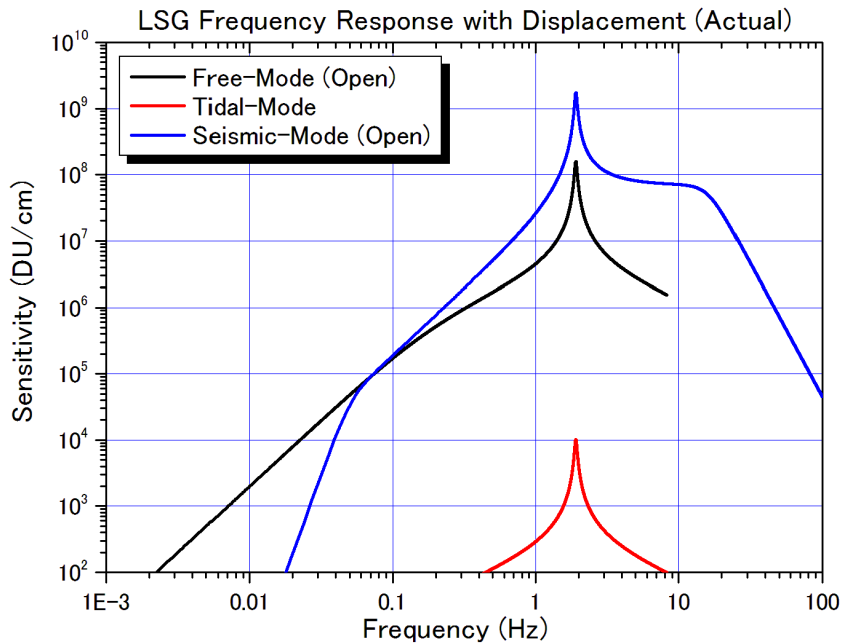


Fig.21 The actual response curves of the LSG with three modes indicated in (DU/cm).

Comparison with the response curves of the LSG and those of the PSE in Figure 6 shows that the LSG can observe the lunar ground motion as well as PSE in seismic mode around 1 Hz.

[References]

(Apollo Passive Seismic Experiment)

[1]G. Latham, M. Ewing, F. Press, G. Sutton, J. Dorman, Y. Nakamura, N. Toksoz, R. Wiggins, R. Kovach
Passive Seismic Experiment; in Apollo 12 Preliminary Science Report
NASA SP-214, (1970) p.39-53

[2]G. Latham, M. Ewing, F. Press, G. Sutton
The Apollo Passive Seismic Experiment
Science (1969) vol.165, No.3690, p.241-250

[3]P. Horvath
Analysis of Lunar Seismic Signals – Determination of Instrumental Parameters and Seismic Velocity Distributions –
Doctoral Thesis in the University of Texas at Dallas (1979)

(Apollo Active Seismic Experiment and Lunar Seismic Profiling Experiment)

[4]R. Kovach, J. Watkins, T. Landers
Active Seismic Experiment; in Apollo 14 Preliminary Science Report
NASA SP-272 (1971) p.163-174

[5]R. Kovach, J. Watkins, P. Talwani
Active Seismic Experiment; in Apollo 16 Preliminary Science Report
NASA SP-315 (1972) p.10-1 – 10-14

[6]Active Seismic Experiment (NASA Experiment S-033)
In Apollo Scientific Experiments Data Handbook, NASA TM X-58131
JSC-09166 (1974) p.5-1 – 5-25

[7]R. Kovach, J. Watkins, P. Talwani
Lunar Seismic Profiling Experiment; in Apollo 17 Preliminary Science Report
NASA SP-330 (1973) p.10-1 – 10-12

[8]M. Brzostowski, A. Brzostowski
Archiving the Apollo Active Seismic Data
The Landing Edge (2009) p.414-416

(Apollo Lunar Surface Gravimeter)

[9]J. Giganti, J. Larson, J. Richard, J. Weber
Lunar Surface Gravimeter Experiment; in Apollo 17 Preliminary Science Report
NASA SP-330 (1973) p.12-1 – 12-4

[10]J. Giganti, J. Larson, J. Richard, R. Tobins, J. Weber
Lunar Surface Gravimeter Experiment Final Report

Contract NASA 9-5886 (1977) p.1-21

[11]Lunar Surface Gravimeter

In Apollo Lunar Surface Experiments Package; Apollo 17 ALSEP Familiarization Course Handout
Contract NAS 9-5829 (1972) p.97-134

[12]J. Weber, J. Larson

Lunar Surface Gravimeter Experiment (LSGE)
Report in Physics Department of University of Maryland